Article

Site-Specific Insertion of 3-Aminotyrosine into Subunit 2 of *E. coli* Ribonucleotide Reductase: Direct Evidence for Involvement of Y˙ and Y in Radical Propagation

Mohammad R. Seyedsayamdost, Jianming Xie, Clement T. Y. Chan, Peter G. Schultz, and JoAnne Stubbe

J. Am. Chem. Soc., **2007**, 129 (48), 15060-15071 • DOI: 10.1021/ja076043y

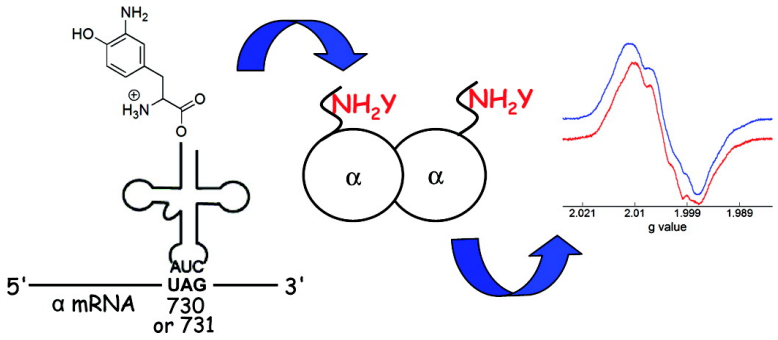

More About This Article

Additional resources and features associated with this article are available within the HTML version:

- Supporting Information
- Links to the 3 articles that cite this article, as of the time of this article download
- Access to high resolution figures
- Links to articles and content related to this article
- Copyright permission to reproduce figures and/or text from this article

View the Full Text HTML

J|A|C|S
ARTICLES
Published on Web 11/09/2007

Site-Specific Insertion of 3-Aminotyrosine into Subunit α2 of *E. coli* Ribonucleotide Reductase: Direct Evidence for Involvement of Y_{730} and Y_{731} in Radical Propagation

Mohammad R. Seyedsayamdost,[†] Jianming Xie,[§] Clement T. Y. Chan,[†] Peter G. Schultz,[§] and JoAnne Stubbe*[,†,‡]

Contribution from the Department of Chemistry and Biology, Massachusetts Institute of Technology, 77 Massachusetts Avenue, Cambridge, Massachusetts 02139-4307, and Department of Chemistry and the Skaggs Institute for Chemical Biology, The Scripps Research Institute, 10550 North Torrey Pines Road, La Jolla, California 92037

Received August 10, 2007; E-mail: stubbe@mit.edu

Abstract: *E. coli* ribonucleotide reductase (RNR) catalyzes the production of deoxynucleotides using complex radical chemistry. Active RNR is composed of a 1:1 complex of two subunits: α2 and β2. α2 binds nucleoside diphosphate substrates and deoxynucleotide/ATP allosteric effectors and is the site of nucleotide reduction. β2 contains the stable diiron tyrosyl radical (Y_{122}•) cofactor that initiates deoxynucleotide formation. This process is proposed to involve reversible radical transfer over >35 Å between the Y_{122}• in β2 and C_{439} in the active site of α2. A docking model of α2β2, based on structures of the individual subunits, suggests that radical initiation involves a pathway of transient, aromatic amino acid radical intermediates, including Y_{730} and Y_{731} in α2. In this study the function of residues Y_{730} and Y_{731} is investigated by their site-specific replacement with 3-aminotyrosine (NH_2Y). Using the in vivo suppressor tRNA/aminoacyl-tRNA synthetase method, $Y_{730}NH_2Y$-α2 and $Y_{731}NH_2Y$-α2 have been generated with high fidelity in yields of 4−6 mg/g of cell paste. These mutants have been examined by stopped flow UV−vis and EPR spectroscopies in the presence of β2, CDP, and ATP. The results reveal formation of an NH_2Y radical (NH_2Y_{730}• or NH_2Y_{731}•) in a kinetically competent fashion. Activity assays demonstrate that both NH_2Y-α2s make deoxynucleotides. These results show that the NH_2Y• can oxidize C_{439} suggesting a hydrogen atom transfer mechanism for the radical propagation pathway within α2. The observed NH_2Y• may constitute the first detection of an amino acid radical intermediate in the proposed radical propagation pathway during turnover.

Introduction

In all organisms, ribonucleotide reductases (RNRs) catalyze the conversion of nucleotides to 2′-deoxynucleotides, providing the precursors required for DNA biosynthesis and repair.[1−3] The mechanism of nucleotide reduction is conserved in all RNRs and requires formation of a transient active site thiyl radical (C_{439}•, *E. coli* RNR numbering used throughout the text).[4,5] However, the mechanism of active-site thiyl radical generation, the radical initiation event, is not conserved and provides the basis for distinction between four classes of RNRs.[6−9] A major unresolved mechanistic issue is that of thiyl radical formation in class I RNRs and presumably in the recently identified class IV RNR. In this paper, we report site-specific incorporation of 3-aminotyrosine (NH_2Y) into one of the subunits of *E. coli* RNR and present the insights provided by these mutants into the mechanism of radical initiation.

The *E. coli* class I RNR consists of two homodimeric subunits, α2 and β2, which form an active 1:1 complex during turnover.[10−12] α2 is the business end of the complex. It contains the active site where thiyl radical-mediated nucleotide reduction occurs, as well as multiple allosteric effector binding sites which modulate substrate specificity and turnover rate.[13] β2 houses the stable diferric tyrosyl radical (Y_{122}•)[14−16] cofactor which is required for formation of the transient C_{439}• in the active site of α2.[4−6] The structures of α2[6,17] and β2[18,19] have been solved,

[†] Department of Chemistry, Massachusetts Institute of Technology.
[‡] Department of Biology, Massachusetts Institute of Technology.
[§] The Scripps Research Institute.

(1) Stubbe, J.; van der Donk, W. A. *Chem. Rev.* **1998**, *98*, 705.
(2) Jordan, A.; Reichard, P. *Annu. Rev. Biochem.* **1998**, *67*, 71.
(3) Nordlund, P.; Reichard, P. *Annu. Rev. Biochem.* **2006**, *75*, 681.
(4) Stubbe, J. *J. Biol. Chem.* **1990**, *265*, 5329.
(5) Stubbe, J. *Proc. Natl. Acad. Sci. U.S.A.* **1998**, *95*, 2723.
(6) Uhlin, U.; Eklund, H. *Nature* **1994**, *370*, 533.
(7) Licht, S.; Gerfen, G. J.; Stubbe, J. *Science* **1996**, *271*, 477.
(8) Logan, D. T.; Andersson, J.; Sjöberg, B.-M.; Nordlund, P. *Science* **1999**, *283*, 1499.
(9) Jiang, W.; Yun, D.; Saleh, L.; Barr, E. W.; Xing, G.; Hoffart, L. M.; Maslak, M. A.; Krebs, C.; Bollinger, J. M., Jr. *Science* **2007**, *316*, 1188.
(10) Brown, N. C.; Reichard, P. *J. Mol. Biol.* **1969**, *46*, 25.
(11) Thelander, L. *J. Biol. Chem.* **1973**, *248*, 4591.
(12) Wang, J.; Lohman, G. J.; Stubbe, J. *Proc. Natl. Acad. Sci. U.S.A.* **2007**, *104*, 14324.
(13) Brown, N. C.; Reichard, P. *J. Mol. Biol.* **1969**, *46*, 39.
(14) Ehrenberg, A.; Reichard, P. *J. Biol. Chem.* **1972**, *247*, 3485.
(15) Sjöberg, B.-M.; Reichard, P.; Gräslund, A.; Ehrenberg, A. *J. Biol. Chem.* **1978**, *253*, 6863.
(16) Reichard, P.; Ehrenberg, A. *Science* **1983**, *221*, 514.
(17) Eriksson, M.; Uhlin, U.; Ramaswamy, S.; Ekberg, M.; Regnstrom, K.; Sjöberg, B.-M.; Eklund, H. *Structure* **1997**, *5*, 1077.

10.1021/ja076043y CCC: $37.00

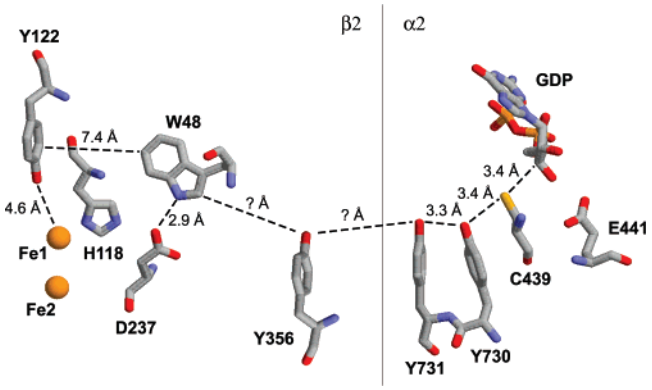

Figure 1. The putative radical initiation pathway generated from the docking model of α2 and β2.[6] Y_{356} is not visible in any structures because it lies on the disordered C-terminal tail of β2. Therefore, the distances from Y_{356} to β2-W_{48} and to α2-Y_{731} are not known. Distances on the α2 side are from the structure determined by Uhlin and Eklund[6] and those on the β2 side are from the high-resolution structure of oxidized β2.[19]

and a structure containing both subunits has also been reported.[20] A structure of the active α2β2 complex, however, has remained elusive. From the individual structures of α2 and β2, Uhlin and Eklund have generated a docking model of the α2β2 complex based on shape and charge complementarities and conserved residues.[6] This model suggests that the Y_{122}• in β2 is located >35 Å away from C_{439} in α2 (Figure 1).[21−23] Radical propagation over this long distance requires the involvement of transient amino acid radical intermediates.[24−26] The residues proposed to participate in this pathway are universally conserved in all class I RNRs.

Evidence in support of the long distance between Y_{122}• and C_{439} has recently been obtained from pulsed electron−electron double resonance spectroscopic measurements[27] with a mechanism-based inhibitor.[28−32] The distance obtained from this study is consistent with the docking model and establishes that a large conformational change, that positions Y_{122}• in β2 adjacent to C_{439} in α2, does not occur.[32]

To examine the validity of the proposed pathway, site-directed mutagenesis[33,34] and complementation studies[35] have been carried out. These studies demonstrate that each residue in Figure 1 plays an important role in RNR function. However, the absence of activity in these mutants precludes mechanistic investigations.[33,34]

At present, evidence for the involvement of only one of the proposed pathway residues, Y_{356}, is substantial. Demonstration of the involvement of this residue is particularly important as it resides within a disordered region of β2 and hence its distance to W_{48} in β2 and to Y_{731} in α2 is long and not known (Figure 1). We have recently been able incorporate unnatural amino acids at residue 356 using expressed protein ligation methods, to generate mechanistically informative mutants.[36,37] In one variant, Y_{356} was replaced with the radical trap 3,4-dihydroxyphenylalanine (DOPA).[38] Studies with $DOPA_{356}$-β2 and α2 in the presence of substrate and/or effector showed formation of a DOPA radical (DOPA•) in a kinetically competent fashion directly demonstrating that residue 356 is redox-active.[38] We have also employed a DOPA heterodimer, DOPA-$\beta\beta'$ (where the β'-monomer lacks the C-terminal 22 residues), to show reverse hole migration from residue 356 to Y_{122}.[39] The most compelling evidence, however, for the redox-active role of Y_{356} has come from a series of semisynthetic β2s in which fluorotyrosine analogues (F_nYs, n = 2, 3, or 4) were site-specifically inserted at this residue.[40−43] These F_nY_{356}-β2 derivatives have allowed systematic modulation of the reduction potential and pK_a of this residue, key to unraveling the role of proton-coupled electron transfer within the pathway.[21,40] Activity assays of F_nY_{356}-β2s showed that radical initiation, and thus nucleotide reduction, is turned on or off on the basis of the reduction potential difference between the F_nY and Y.[43] In addition, modulation of the pK_a in F_nY-β2s, allowed us to show that there was no obligate coupling between the electron and proton at this residue during radical transport.[43] Studies using semisynthetic β2s have thus defined the function and mechanism of residue 356 in radical propagation.

In contrast, the roles of α2 residues Y_{730} and Y_{731} in radical propagation are still ill-defined. Mutagenesis studies have demonstrated their importance in RNR function.[34,44,45] However, as with residue Y_{356} in β2, the inactivity of these mutants (Y_{730}F-α2 and Y_{731}F-α2) precluded mechanistic interrogation of the role of Y_{730} and Y_{731} in radical propagation. Furthermore, incorporation of unnatural amino acids into α2 is not feasible by expressed protein ligation given the location of these residues. We have thus sought an alternative method to site−specifically incorporate unnatural amino acids.

We now report evolution of an NH_2Y-specific *Methanococcus jannaschii* aminoacyl-tRNA synthetase (NH_2Y-RS) and its use in vivo with the appropriate *M. jannaschii* amber suppressor tRNA, to incorporate NH_2Y at residues Y_{730} and Y_{731} of the

(18) Nordlund, P.; Sjöberg, B.-M.; Eklund, H. *Nature* **1990**, *345*, 593.
(19) Högbom, M.; Galander, M.; Andersson, M.; Kolberg, M.; Hofbauer, W.; Lassmann, G.; Nordlund, P.; Lendzian, F. *Proc. Natl. Acad. Sci.* **2003**, *100*, 3209.
(20) Uppsten, M.; Farnegardh, M.; Domkin, V.; Uhlin, U. *J. Mol. Biol.* **2006**, *359*, 365.
(21) Stubbe, J.; Nocera, D. G.; Yee, C. S.; Chang, M. C. Y. *Chem. Rev.* **2003**, *103*, 2167.
(22) Stubbe, J.; Riggs-Gelasco, P. *Trends Biochem. Sci.* **1998**, *23*, 438.
(23) Lawrence, C. C.; Stubbe, J. *Curr. Opin. Chem. Biol.* **1998**, *2*, 650.
(24) Marcus, R. A.; Sutin, N. *Biochim. Biophys. Acta* **1985**, *811*, 265.
(25) Moser, C. C.; Keske, J. M.; Warncke, K.; Farid, R. S.; Dutton, P. L. *Nature* **1992**, *355*, 796.
(26) Gray, H. B.; Winkler, J. R. *Annu. Rev. Biochem.* **1996**, *65*, 537.
(27) Bennati, M.; Weber, A.; Antonic, J.; Perlstein, D. L.; Robblee, J.; Stubbe, J. *J. Am. Chem. Soc.* **2005**, *125*, 14988.
(28) Thelander, L.; Larsson, B.; Hobbs, J.; Eckstein, F. *J. Biol. Chem.* **1976**, *251*, 1398.
(29) Sjöberg, B.-M.; Gräslund, A.; Eckstein, F. *J. Biol. Chem.* **1983**, *258*, 8060.
(30) Salowe, S.; Bollinger, J. M., Jr.; Ator, M.; Stubbe, J.; McCraken. J.; Peisach, J.; Samano, M. C.; Robins, M. J. *Biochemistry* **1993**, *32*, 12749.
(31) Fritscher, J.; Artin, E.; Wnuk, S.; Bar, G.; Robblee, J. H.; Kacprzak, S.; Kaupp, M.; Griffin, R. G.; Bennati, M.; Stubbe, J. *J. Am. Chem. Soc.* **2005**, *127*, 7729.
(32) Bennati, M.; Robblee, J. H.; Mugnaini, V.; Stubbe, J.; Freed, J. H.; Borbat, P. *J. Am. Chem. Soc.* **2005**, *127*, 15014.
(33) Climent, I.; Sjöberg, B.-M.; Huang, C. Y. *Biochemistry* **1992**, *31*, 4801.
(34) Ekberg, M.; Sahlin, M.; Eriksson, M.; Sjöberg, B.-M. *J. Biol. Chem.* **1996**, *271*, 20655.
(35) Ekberg, M.; Birgander, P.; Sjöberg, B.-M. *J. Bacteriol.* **2003**, *185*, 1167.
(36) Yee, C. S.; Seyedsayamdost, M. R.; Chang, M. C.; Nocera, D. G.; Stubbe, J. *Biochemistry* **2003**, *42*, 14541.
(37) Seyedsayamdost, M. R.; Yee, C. S.; Stubbe, J. *Nat. Protoc.* **2007**, *2*, 1225.
(38) Seyedsayamdost, M. R.; Stubbe, J. *J. Am. Chem. Soc.* **2006**, *128*, 2522.
(39) Seyedsayamdost, M. R.; Stubbe, J. *J. Am. Chem. Soc.* **2007**, *129*, 2226.
(40) Seyedsayamdost, M. R.; Reece, S. Y.; Nocera, D. G.; Stubbe, J. *J. Am. Chem. Soc.* **2006**, *128*, 1569.
(41) Yee, C. S.; Chang, M. C.; Ge, J.; Nocera, D. G.; Stubbe, J. *J. Am. Chem. Soc.* **2003**, *125*, 10506.
(42) Reece, S. Y.; Seyedsayamdost, M. R.; Stubbe, J.; Nocera, D. G. *J. Am. Chem. Soc.* **2006**, *128*, 13654.
(43) Seyedsayamdost, M. R.; Yee, C. S.; Reece, S. Y.; Nocera, D. G.; Stubbe, J. *J. Am. Chem. Soc.* **2006**, *128*, 1562.
(44) Chang, M. C.; Yee, C. S.; Stubbe, J.; Nocera, D. G. *Proc. Natl. Acad. Sci. U.S.A.* **2004**, *101*, 6882.
(45) Reece, S. Y.; Seyedsayamdost, M. R.; Stubbe, J.; Nocera, D. G. *J. Am. Chem. Soc.* **2007**, *129*, 8500.

Scheme 1. One-Electron Oxidation of NH_2Y[51]

α2 subunit.[46−50] NH_2Y was chosen as a probe because its reduction potential (0.64 V at pH 7.0, Scheme 1)[51] is 0.19 V lower than that of Y, indicating that it might act as a radical trap, similar to DOPA, and directly report on participation of residues Y_{730} and Y_{731} in hole migration (Figure 1). Furthermore NH_2Y is more stable to oxidation than DOPA, making it a more practical target.[51,52] Using this methodology, 100 mg quantities of each NH_2Y-α2 have been generated. Incubation of Y_{730}-NH_2Y-α2 (or $Y_{731}NH_2Y$-α2) with β2, substrate and allosteric effector, results in formation of an NH_2Y radical (NH_2Y•) in a kinetically competent fashion as demonstrated by stopped-flow (SF) UV−vis and EPR spectroscopy. Unexpectedly, the NH_2Y-α2s retain the ability to make deoxynucleotides, suggesting that the NH_2Y•observed, occurs during radical propagation in a complex that is competent in nucleotide reduction. These results suggest that direct hydrogen atom transfer is the operative mechanism for hole migration within α2.

Materials and Methods

Materials. Luria Bertani (LB) medium, BactoAgar, 2YT medium, and small and large diameter (100 and 150 mm) Petri dish plates were obtained from Becton-Dickinson. NH_2Y, M9 salts, tetracycline (Tet), kanamycin (Kan), ampicillin (Amp), L-arabinose (L-Ara), chloramphenicol (Cm), L-leucine (Leu), D-biotin, thiamine HCl, ATP, cytidine-5′-diphosphate (CDP), NADPH, ethylenediamine tetraacetic acid (EDTA), glycerol, Bradford Reagent, Sephadex G-25, phenylmethanesulfonyl fluoride (PMSF), streptomycin sulfate, hydroxyurea, 2′-deoxycytidine, and 2′-deoxyguanidine-5′-triphosphate (dGTP) were purchased from Sigma-Aldrich. Isopropyl-β-D-thiogalactopyranoside (IPTG), DL-dithiothreitol (DTT) and T4 DNA ligase were from Promega. DH10B competent cells and oligonucleotides were from Invitrogen. Site-directed mutagenesis was carried out with the Quikchange Kit from Stratagene. Calf-intestine alkaline phosphatase (CAP, 20 U/μL) was from Roche. KpnI and XboI restriction enzymes were from NEB. The pTrc vector was a generous gift of Prof. Sinskey (Department of Biology, M.I.T.). The purification of *E. coli* thioredoxin[53] (TR, 40 units/mg), *E. coli* thioredoxin reductase[54] (TRR, 1400 units/mg), and wild-type (wt) β2[55] (6200−7200 nmol/min•mg, 1−1.2 radicals per dimer) have been described. The concentrations of α2, $Y_{730}NH_2Y$-α2, and $Y_{731}NH_2Y$-α2 were determined using $\epsilon_{280\ nm} = 189\ mM^{-1}\ cm^{-1}$. Glycerol minimal media leucine (GMML) contains final concentrations of 1% (v/v) glycerol, 1 × M9 salts, 0.05% (w/v) NaCl, 1 mM $MgSO_4$, 0.1 mM $CaCl_2$, and 0.3 mM L-leucine. RNR assay buffer consists of 50 mM Hepes, 15 mM $MgSO_4$, 1 mM EDTA, pH 7.6.

Qualitative Assay for Cellular Uptake of NH_2Y by LC-MS. The uptake assay was performed as previously described with minor modifications.[48] DH10B *E. coli* cells were grown to saturation at 37 °C in GMML in the presence of 1 mM NH_2Y and 0.1 mM DTT and subsequently harvested and lysed as outlined previously. Chromatography of the crude extract was performed on a Zorbax SB-C18 (5 μm, 4.6 × 150 mm) column with a linear gradient from 5% to 25% MeCN in 0.1% TFA solution over 8 min at 0.5 mL/min. Under these conditions, NH_2Y elutes at ~13% MeCN. For HPLC−ESI-MS analysis, NH_2Y standard solutions were prepared in water.

Directed Evolution of NH_2Y-RS in *E. coli*. Positive and negative selection cycles were carried out as detailed previously.[48] Briefly, plasmid pBK-JYRS encodes a library of *M. jannaschii* TyrRS variants, which are randomized at six residues within 6.5 Å of the Tyr binding cleft, under the control of the *E. coli* GlnRS promoter and contains a Kan^R marker.[46] Plasmid pREP/YC-J17 was used for positive selections;[56] it encodes a chloramphenicol acetyl transferase (CAT) gene with a nonessential amber mutation, $Asp_{112}TAG$, and a T7 RNA polymerase (T7 RNAP) gene with two nonessential amber mutations, Met_1TAG and $Gln_{107}TAG$. It also contains a gene for the cognate mutant $tRNA_{CUA}$ ($mutRNA_{CUA}$) that is charged by the library of TyrRSs, a GFPuv gene, the expression of which is driven by T7 RNAP and a Tet^R marker. Plasmid pLWJ17B3 was used for negative selections;[57,58] it encodes a toxic barnase gene with three nonessential amber mutations, Gln_2TAG, $Asp_{44}TAG$, and $Gly_{65}TAG$, under the control of an *Ara* promoter. It also contains the $mutRNA_{CUA}$ gene and an Amp^R marker (Table 1).

In each positive selection round, the pBK-JYRS plasmid library, containing the library of mutant TyrRSs, was transformed into *E. coli* DH10B competent cells containing plasmid pREP/YC-J17 by electroporation.[48] The cells were recovered in SOC medium and grown at 37 °C for 1 h. They were then washed twice with GMML and plated onto 6−8 GMML agar plates (150 mm) containing 12 μg/mL Tet, 25 μg/mL Kan, 60 μg/mL chloramphenicol (Cm), 1 mM NH_2Y, and 100 μM DTT. DTT was included in all solutions or plates that contained NH_2Y to maintain a reducing environment. Plates were incubated at 37 °C for 72 h. Surviving cells were scraped from the plates and pooled into GMML liquid medium. The cells were then subjected to plasmid isolation using the Qiagen Miniprep Kit. The pBK-JYRS library (~3 kb) was separated from pREP/YC-J17 (~10 kb) by agarose gel electrophoresis and extracted from the gel with the Qiagen gel extraction kit. Plasmid DNA was quantitated using $OD_{260\ nm}$.

To perform a negative selection, plasmid DNA isolated from the positive selection was transformed by electroporation into *E. coli* DH10B competent cells containing pLWJ17B3.[48] The cells were recovered in SOC medium, shaken at 37 °C for 1 h, and plated onto LB agar plates containing 100 μg/mL Amp, 50 μg/mL Kan and 0.2% L-Ara. The plates were incubated at 37 °C for 10−12 h. Surviving cells were recovered and plasmid isolation was performed as described above.

After a total of six rounds (three positive and three negative selections), the fourth positive selection was performed by spreading cells onto two sets of plates. One set contained NH_2Y/DTT as described for the positive rounds, the other contained only DTT. The two sets of plates were examined for differences in green fluorescence stemming from GFPuv, the expression of which is driven by T7 RNAP on the positive selection plasmid (Table 1). A total of 48 single colonies were selected from the plates which contained NH_2Y/DTT and inoculated into 100 μL of GMML in a 96-well plate. One μL from each resulting cell suspension was plated onto two sets of GMML agar plates containing 0, 20, 40, 60, 80, and 110 μg/mL Cm and 0.1 mM DTT in the presence and absence of 1 mM NH_2Y. Plates were incubated at 37 °C for 72−120 h. Candidate clones are able to survive on plates

(46) Wang, L.; Brock, A.; Herberich, B.; Schultz, P. G. *Science* **2001**, *292*, 498.
(47) Wang, L.; Schultz, P. G. *Angew. Chem., Int. Ed. Engl.* **2004**, *44*, 34.
(48) Xie, J.; Schultz, P. G. *Methods* **2005**, *36*, 227.
(49) Wang, L.; Xie, J.; Schultz, P. G. *Annu. Rev. Biophys. Biomol. Struct.* **2006**, *35*, 225.
(50) Xie, J.; Schultz, P. G. *Nat. Rev. Mol. Cell Biol.* **2006**, *7*, 775.
(51) DeFelippis, M. R.; Murthy, C. P.; Broitman, F.; Weinraub, D.; Faraggi, M.; Klapper, M. H. *J. Phys. Chem.* **1991**, *95*, 3416.
(52) Jovanovic, S. J.; Steenken, S.; Tosic, M.; Marjanovic, B.; Simic, M. G. *J. Am. Chem. Soc.* **1994**, *116*, 4846.
(53) Chivers, P. T.; Prehoda, K. E.; Volkman, B. F.; Kim, B.-M.; Markley, J. L.; Raines, R. T. *Biochemistry* **1997**, *36*, 14985.
(54) Russel, M.; Model, P. *J. Bacteriol.* **1985**, *163*, 238.
(55) Salowe, S. P.; Stubbe, J. *J. Bacteriol.* **1986**, *165*, 363.
(56) Santoro, S. W.; Wang, L.; Herberich, B.; King, D. S.; Schultz, P. G. *Nat. Biotechnol.* **2002**, *20*, 1044.
(57) Wang, L.; Zhang, Z.; Brock, A.; Schultz, P. G. *Proc. Natl. Acad. Sci. U.S.A.* **2003**, *100*, 56.
(58) Chin, J. W.; Martin, A. B.; King, D. S.; Wang, L.; Schultz, P. G. *Proc. Natl. Acad. Sci. U.S.A.* **2002**, *99*, 11020.

Table 1. Vectors Used in This Study

plasmid	description	reference
pBK−JYRS	*M. jannaschii* TyrRS library, Kan^R	46
pREP/YC−J17	positive selection plasmid: CAT ($Asp_{112}TAG$), T7 RNAP (Met_1TAG, $Gln_{107}TAG$), $mutRNA_{CUA}$, GFPuv, Tet^R	56
pLWJ17B3	negative selection plasmid: barnase (Gln_2TAG, $Asp_{44}TAG$, $Gly_{65}TAG$), $mutRNA_{CUA}$, Amp^R	57, 58
pBK−NH_2Y−RS	NH_2Y−RS, Kan^R	this study
pLEIZ	Z−Domain, Cm^R	57, 59
pTrc−*nrdA*	*nrdA* expression vector: *nrdA* ($Tyr_{730}TAG$ or $Tyr_{731}TAG$) with trc promoter, Amp^R	this study
pAC−NH_2Y−RS	NH_2Y−RS, 6 × $mutRNA_{CUA}$, Tet^R	this study
pMJ1−*nrdA*[a]	*nrdA* expression vector: *nrdA* with T7 promoter, Amp^R	60
pBAD−*nrdA*[b]	*nrdA* expression vector: *nrdA* with L−Ara promoter, $mutRNA_{CUA}$, Tet^R	61, this study

[a] pMJ1-*nrdA* expressing wt α2 has been reported. See Supporting Information for TAG codon insertion into the *nrdA* gene of this vector. [b] *nrdA* was cloned into pBAD-JYCUA, which has been described before. See Supporting Information for generation of pBAD-*nrdA* and TAG codon insertion.

with NH_2Y/DTT and high concentrations of Cm (∼100 μg/mL) and emit green fluorescence under UV light, but die on plates without NH_2Y at low concentration of Cm (20 μg/mL). Candidate clones were inoculated into 5 mL of 2YT medium containing 24 μg/mL Tet and 50 μg/mL Kan and grown to saturation. Plasmid DNA was then isolated as described above and analyzed by DNA sequencing. The plasmid containing the NH_2Y-RS gene, which was selected by the procedures above, is pBK-NH_2Y-RS.

Expression of K_7NH_2Y-Z-Domain. The efficiency of NH_2Y incorporation using pBK-NH_2Y-RS was tested using the C-terminally His-tagged Z-domain of protein A (Z-domain), as previously described.[48] pLEIZ,[57,59] which encodes the Z-domain with an amber stop codon at residue 7 and $mutRNA_{CUA}$, and pBK-NH_2Y-RS were co-transformed into BL21(DE3) competent cells. All growths were carried out in the presence of Kan (50 μg/mL) and Cm (35 μg/mL) at 37 °C. A single colony was inoculated into a 5 mL of 2YT medium and grown to saturation (∼13 h). One mL of this saturated culture was diluted into 25 mL of 2YT medium and grown to saturation overnight (∼11 h). Ten mL of this culture were then diluted into each of 2 × 250 mL of GMML medium. When the $OD_{600\ nm}$ reached 0.65 (9 h), one of the cultures was supplemented with NH_2Y and DTT (final concentrations of 1 and 0.1 mM, respectively); the other culture was supplemented only with DTT (0.1 mM). Fifteen min after addition of NH_2Y/DTT (or DTT), IPTG was added to each culture to a final concentration of 1 mM. After 5 h, cells were harvested by centrifugation. Z-domain grown in the presence and absence of NH_2Y was then purified by Ni^{2+} affinity chromatography, as previously described, and subjected to SDS PAGE and MALDI-TOF MS analysis.[48] For MALDI-TOF MS analysis, the Z-domain was exchanged into water by dialysis and mass spectra were subsequently obtained under positive ionization mode at the Scripps Center for Mass Spectrometry.

Cloning of pTrc-*nrdA*. To generate vector pTrc-*nrdA*, the *nrdA* gene was amplified with primers 1 (5′−AT AAT TGG TAC CCA AAA ACA GGT ACG ACA TAC ATG AAT C−3′) and 2 (5′−GCT GCA GGT CGA CTC TAG AGG ATC CCC CCT TCT TAT C−3′) using Pfu Turbo polymerase. The primers contain KpnI and XboI cut sites at the 5′ and 3′ ends of the gene (underlined), respectively. The fragment was purified using the PCR purification kit from Qiagen. The isolated DNA was then incubated with KpnI and XboI, the resulting products separated on an agarose gel, and extracted with the Qiagen gel extraction kit. The gene fragment was ligated into pTrc, which had been cut with the same restriction enzymes. Incubation of the insert-vector in a ratio of 3:1 and ligation with T4 DNA ligase at 16 °C for 30 min resulted in pTrc-*nrdA*.

Expression of wt α2 from vector pTrc-*nrdA* was performed in *E. coli* DH10B cells as previously described for expression from plasmid pMJ1-*nrdA* and yielded 3 g of wet cell paste per L culture.[55,62] Purification of α2 (see below) yielded 10 mg of α2 per g of wet cell paste with >95% purity and a specific activity of 2500 nmol/min·mg as measured by the spectrophotometric RNR assay (see below).

Generation of pTrc-$nrdA_{730}$TAG and pTrc-$nrdA_{731}$TAG. The TAG codon was inserted into position 730 or 731 of the *nrdA* gene in vector pMJ1-*nrdA* using the Stratagene Quickchange kit. Primers 3 (5′−G GTC AAA ACA CTG TAG TAT CAG AAC ACC CG−3′) and 4 (5′−CG GGT GTT CTG ATA CTA CAG TGT TTT GAC C−3′) were used for incorporation of TAG into position 730 of α2. Primers 5 (5′−G GTC AAA ACA CTG TAT TAG CAG AAC ACC CG−3′) and 6 (5′−CG GGT GTT CTG CTA ATA CAG TGT TTT GAC C−3′) were used for incorporation of TAG into position 731 of α2. The mutations were confirmed by sequencing the entire gene at the MIT Biopolymers Laboratory. The $nrdA_{730}$TAG and $nrdA_{731}$TAG genes were then amplified with primers 1 and 2 and ligated into vector pTrc as described above for wt *nrdA*.

Cloning of pAC-NH_2Y-RS. The pAC vector is analogous to vector pSup, which has been described, except that it contains the Tet^R selection marker rather than the Cm^R marker.[63] In addition, pAC-NH_2Y-RS contains the NH_2Y-RS gene under control of *glnS′* promoter and *rrnB* terminator and six copies of the $mutRNA_{CUA}$ gene under control of a *proK* promoter and terminator. To generate pAC-NH_2Y-RS, the NH_2Y-RS gene was subcloned into the pAC vector from pBK-NH_2Y-RS using the PstI and NdeI restriction sites, which are 3′ and 5′ of the NH_2Y-RS gene, respectively.

Expression of $Y_{730}NH_2Y$-α2 and $Y_{731}NH_2Y$-α2. Successful expression of $Y_{730}NH_2Y$-α2 was achieved with the pTrc-$nrdA_{730}$TAG/pAC-NH_2Y-RS expression system, where vector pTrc-$nrdA_{730}$TAG contains the *nrdA* gene with an amber codon at position 730 under control of the *trp/lac* (trc) promoter and *rrnB* terminator and an Amp^R marker. *E. coli* DH10B cells were transformed with vectors pTrc-$nrdA_{730}$TAG and pAC-NH_2Y-RS, and grown at 37 °C on LB/Agar plates containing Amp (100 μg/mL) and Tet (25 μg/mL) for 2 days. All liquid culture growths contained Amp (100 μg/mL) and Tet (25 μg/mL) and were carried out in a shaker/incubator at 37 °C and 200 rpm. A single colony from the plate was inoculated into 5 mL of 2YT medium and grown to saturation (∼2 days). The 5 mL saturated culture was then diluted into 180 mL of 2YT medium and grown to saturation (∼1 day). A 25 mL portion of this culture was then inoculated into each of 6 × 6 L Erlenmeyer flasks, each containing 1 L of GMML medium supplemented with D-biotin (1 μg/mL), thiamine (1 μg/mL), and a 1× heavy-metal stock solution. A 1000× heavy-metal stock solution contains

(59) Zhang, Z.; Wang, L.; Brock, A.; Schultz, P. G. *Angew. Chem., Int. Ed. Engl.* **2002**, *41*, 2840.
(60) Mao, S. S.; Johnston, M. I.; Bollinger, J. M.; Stubbe, J. *Proc. Natl. Acad. Sci. U.S.A.* **1989**, *86*, 1485.
(61) Zhang, Z.; Smith, B. A. C.; Wang, L.; Brock, A.; Cho, C.; Schultz, P. G. *Biochemistry* **2003**, *42*, 6735.
(62) Salowe, S. P. *Ph.D. Thesis.* Massachusetts Institute of Technology, Cambridge, MA, 1992.
(63) Ryu, Y.; Schultz, P. G. *Nat. Methods* **2006**, *3*, 263.

the following per L as described:[64] 500 mg of $MoNa_2O_4 \cdot 2H_2O$, 250 mg of $CoCl_2$, 175 mg of $CuSO_4 \cdot 5H_2O$, 1 g of $MnSO_4 \cdot H_2O$, 8.75 g of $MgSO_4 \cdot 7H_2O$, 1.25 g of $ZnSO_4 \cdot 7H_2O$, 1.25 g of $FeCl_2 \cdot 4H_2O$, 2.5 g of $CaCl_2 \cdot 2H_2O$, 1 g of H_3BO_3, and 1 M HCl. When $OD_{600\ nm}$ reached 0.6 (12−18 h), NH_2Y and DTT were added to final concentrations of 1 and 0.1 mM, respectively. After 15 min, IPTG was added to a final concentration of 1 mM and the growth continued for 4.5 h, at which point the cells were harvested by centrifugation, frozen in liquid N_2, and stored at −80 °C. Typically, 1.5 g of wet cell paste were obtained per L culture. Expression of $Y_{731}NH_2Y$-α2 was carried out in identical fashion using vectors pTrc-*nrdA*$_{731}$TAG and pAC-NH_2Y-RS.

Purification of $Y_{730}NH_2Y$-α2 and $Y_{731}NH_2Y$-α2. NH_2Y-α2s were typically purified from 10 g of wet cell paste. All purification steps were performed at 4 °C. Each g of wet cell paste was resuspended in 5 mL of α2 buffer (50 mM Tris, 1 mM EDTA, pH 7.6) supplemented with 1 mM PMSF and 5 mM DTT. The cells were lysed by passage through a French pressure cell operating at 14 000 psi. After removal of cell debris by centrifugation (15000*g*, 35 min, 4 °C), DNA was precipitated by dropwise addition of 0.2 volumes of α2 buffer containing 8% (w/v) streptomycin sulfate. The mixture was stirred for an additional 15 min, and the precipitated DNA was removed by centrifugation (15000*g*, 35 min, 4 °C). Then, 3.9 g of solid $(NH_4)_2SO_4$ was added per 10 mL of supernatant over 15 min (66% saturation). The solution was stirred for an additional 30 min and the precipitated protein isolated by centrifugation (15000*g*, 45 min, 4 °C). The pellet was redissolved in a minimal volume of α2 buffer and desalted using a Sephadex G-25 column (1.5 cm × 25 cm, 45 mL). The desalted protein was loaded at a flow rate of 0.5 mL/min directly onto a dATP column (1.5 cm × 4 cm, 6 mL), which had been equilibrated in α2 buffer. The column was washed with 10 column volumes of α2 buffer. NH_2Y-α2 was then eluted in 3−4 column volumes of α2 buffer containing 10 mM of ATP, 15 mM $MgSO_4$, and 10 mM DTT. ATP was subsequently removed by Sephadex G-25 chromatography. The protein was flash-frozen in small aliquots in liquid N_2 and stored at −80 °C. Typically 4−6 mg of pure NH_2Y-α2 were obtained per g of wet cell paste.

Reaction of NH_2Y-α2 with *β*2, CDP, and ATP Monitored by EPR Spectroscopy. Prereduced wt-α2 or NH_2Y-α2s were generated by incubating each variant (40 μM) with 35 mM DTT at room temperature for 40 min. Hydroxyurea and additional DTT were added to final concentrations of 15 mM, and the incubation continued at room temperature for an additional 20 min. Each protein was then desalted on a Sephadex G-25 column (1.5 × 25 cm, 45 mL), which had been equilibrated in assay buffer (see Materials).

Prereduced NH_2Y-α2 and ATP were mixed with wt *β*2 and CDP in assay buffer to give final concentrations 20−24 μM, 3 mM, 20−24 μM, and 1 mM, respectively. The reaction was hand-quenched in liquid N_2 from 10 s to 12 min. EPR spectra were recorded at 77 K in the Department of Chemistry Instrumentation Facility on a Bruker ESP-300 X-band spectrometer equipped with a quartz finger dewar filled with liquid N_2. EPR parameters were as follows: microwave frequency = 9.34 GHz, power = 30 μW, modulation amplitude = 1.5 G, modulation frequency = 100 kHz, time constant = 5.12 ms, scan time = 41.9 s. Analysis of the resulting spectra was carried out using WinEPR (Bruker) and an in-house written program in Excel. These programs facilitate fractional subtraction of the unreacted Y_{122}• signal from the recorded spectrum, yielding the spectrum of NH_2Y•-α2. The ratio Y• and NH_2Y• signals was assessed by comparing the double integral intensity of each trace. EPR spin quantitation was carried out using Cu^{II} as standard.[65]

Kinetics of NH_2Y•-α2 Formation with *β*2, CDP, and ATP by Stopped-Flow (SF) UV−Visible Spectroscopy. SF kinetics was performed on an Applied Photophysics DX. 17MV instrument equipped with the Pro-Data upgrade using PMT detection at λs indicated in figure legends. The temperature was maintained at 25 °C with a Lauda RE106 circulating water bath. Prereduced $Y_{730}NH_2Y$-α2 (or $Y_{731}NH_2Y$-α2) and ATP in one syringe were mixed in a 1:1 ratio with wt *β*2 and CDP from a second syringe to yield final concentrations of 8−10 μM, 3 mM, 8−10 μM, and 1 mM, respectively, in assay buffer. Data were collected in split time-base mode. Time courses shown are the average of at least six individual traces. For point-by-point reconstruction of the $Y_{730}NH_2Y$•-α2 and $Y_{731}NH_2Y$•-α2 absorption profiles, 2−4 traces were averaged between 305 and 365 nm in 5 nm intervals. The absorption change was corrected for the absorption of Y_{122}• in this region, on the basis of the published ε at these λs,[66−68] and then plotted against λ. Calculation of the ε for $Y_{730}NH_2Y$•-α2 (10500 M^{-1} cm^{-1}) and $Y_{731}NH_2Y$•-α2 (11000 M^{-1} cm^{-1}) were performed using the ε of Y_{122}• ($\epsilon_{410\ nm}$ = 3700 M^{-1} cm^{-1})[68] and assuming that consumption of each mole of Y_{122}• leads to formation of one mole of NH_2Y• in α2. Curve fitting was performed with OriginPro or KaleidaGraph Software.

Spectrophotometric and Radioactive Activity Assays for RNR. The spectrophotometric and radioactive RNR assays were performed as described before.[36,43] The concentration of NH_2Y-α2 was 0.2, 1, or 3 μM; *β*2 was present at a 5-fold molar excess. [5-^{3}H]-CDP (1190 cpm/nmol) was used in the radioactive assay.

Reaction of NH_2Y-α2 with *β*2, N_3ADP, and dGTP Monitored by EPR Spectroscopy. 2′-Azido-2′-deoxyadenosine-5′-diphosphate (N_3ADP) was previously prepared by Scott Salowe.[62] Prereduced $Y_{730}NH_2Y$-α2 ($Y_{731}NH_2Y$-α2 or wt α2) and dGTP were mixed with wt *β*2 and N_3ADP in assay buffer to yield final concentrations of 20 μM, 1 mM, 20 μM, and 250 μM, respectively. The reaction was hand-quenched in liquid N_2 after 20 s. EPR data acquisition and spin quantitation with Cu^{II} were performed as described above. The resulting spectra were analyzed using WinEPR (Bruker) and an in-house written Excel program. Deconvolution of the three signals observed in these experiments was performed by first subtracting the N• signal which has been reported and was reproduced here with the wt α2/*β*2 reaction. Then, unreacted Y_{122}• was subtracted from this spectrum, yielding the NH_2Y•-α2 spectrum. The ratio of the three signals was assessed by comparing the double integral intensity of each trace.

Results

Toxicity and Uptake of NH_2Y. Evolution of an NH_2Y-specific aminoacyl-tRNA synthetase (RS) requires that NH_2Y is taken up by *E. coli*, that it is not toxic, and that it is not incorporated into proteins by any endogenous RSs. All three requirements were met by NH_2Y. When DH10B *E. coli* cells were grown in liquid GMML medium in the presence of NH_2Y (1 mM) or NH_2Y and DTT (1 mM and 0.1 mM, respectively), NH_2Y was observed in all cell extracts as judged by HPLC and ESI-MS (data not shown).[48] Toxicity of NH_2Y was assessed by growing DH10B *E. coli* cells in liquid GMML medium and on Agar plates in the presence of NH_2Y or NH_2Y/DTT. Growth rates were not significantly affected by the presence of NH_2Y. The presence of DTT however, caused cells to grow at a rate 25−35% more slowly than those in the presence of only NH_2Y or absence of NH_2Y/DTT (data not shown).

Evolution of an NH_2Y-Specific RS. The Schultz lab has developed a robust in vivo method for incorporation of unnatural amino acids into any target protein.[46−50] In this method, the RS is selected from a library of *M. jannaschii* TyrRS mutants. A cognate amber suppressor *M. jannaschii* tRNA, mutRNA$_{CUA}$,

(64) Farrell, I. S.; Toroney, R.; Hazen, J. L.; Mehl, R. A.; Chin, J. W. *Nat. Methods* **2005**, *2*, 377.
(65) Palmer, G. *Methods Enzymol.* **1967**, *10*, 595.
(66) Gräslund, A.; Sahlin, M.; Sjöberg, B.-M. *Environ. Health Perspect.* **1985**, *64*, 139.
(67) Nyholm, S.; Thalander, L.; Gräslund, A. *Biochemistry* **1993**, *32*, 11569.
(68) Bollinger, J. M., Jr.; Tong, W. H.; Ravi, N.; Huynh, B. H.; Edmondson, D. E.; Stubbe, J. *Methods Enzymol.* **1995**, *258*, 278−303.

does not require modification as the region of interaction between mutRNA$_{CUA}$ and the RSs in the library is not varied.[69] Iterative rounds of positive and negative selections are carried out on the RS library which has been randomized at six residues in and around the Y binding cleft: Tyr32, Leu65, Phe108, Gln109, Asp158, and Leu162. The positive selection is based on suppression of an amber stop codon at a permissive site in the CAT gene in the presence of NH_2Y/DTT and the cognate tRNA (Table 1).[46] Surviving clones carry RSs that are functional with the host cell translation machinery and incorporate NH_2Y or other amino acids in response to the amber stop codon. The negative selection is based on lack of suppression of three amber codons in the toxic barnase gene in the absence of NH_2Y (Table 1).[70] Surviving clones carry RSs that do not incorporate any natural amino acids in response to the amber stop codon.

After seven selection cycles, 48 colonies were examined for their ability to suppress the amber stop codon. Single colonies containing pBK-NH_2Y-RS and pREP/YC-J17 were picked from the last positive selection (seventh round) and plated on GMML agar containing variable concentrations of Cm (0−110 μg/mL) in the presence or absence of NH_2Y. Ability to grow with NH_2Y/DTT indicates that the amber codon in the CAT gene is suppressed by incorporation of NH_2Y. Further, the amber codon in the T7 RNAP gene is suppressed in a similar fashion and drives expression of GFPuv, resulting in emission of green fluorescence, when the cells are irradiated with UV light. The desired colonies are those that grow in high concentrations of Cm (~100 μg/mL) and NH_2Y/DTT and emit green fluorescence upon irradiation but die at low Cm concentrations (~20 μg/mL) in the absence of NH_2Y. Of the 48 colonies tested, 2 met these criteria and were pursued further.

DNA sequencing of the plasmids from these colonies revealed identical RSs with the following residues at the randomized positions: Gln32, Glu65, Gly108, Leu109, Ser158, and Tyr162. Interestingly, residue 32, a Tyr in wt *M. jannaschii* TyrRS and positioned within 2 Å of the C-atom ortho to the hydroxyl group of bound Tyr ligand, is a Gln in the selected RS.[71,72] The crystal structure of wt *M. jannaschii* TyrRS suggests that the Gln allows accommodation of the *o*-NH_2 group and perhaps provides favorable hydrogen-bonding interactions. The RS identified from these clones was used for all subsequent experiments.

Expression of K_7NH_2Y-Z-Domain. To test the efficiency and fidelity of NH_2Y incorporation with the selected RS, the C-terminally His-tagged Z-domain protein (Z-domain), with an amber stop codon at the permissive Lys7 residue, served as a model.[57,73] Expression in the presence of NH_2Y/DTT in GMML medium, yielded 5 mg of Z-domain per L culture after purification. SDS PAGE analysis (Figure 2, inset) demonstrated that in the absence of NH_2Y, the amount of Z-domain protein expressed was below the level of detection. The purified protein was subjected to MALDI-TOF MS analysis. Previous studies have shown that the Z-domain is post-translationally modified by removal of the N-terminal Met followed by acetylation of the resulting N-terminal amino acid.[57] Accordingly, MALDI-TOF MS analysis of Z-domain expressed in the presence of NH_2Y/DTT revealed four peaks with MW = 7812, 7854, 7943, and 7985 Da (Figure 2). These features correspond to K_7NH_2Y-Z-domain minus the first Met (MW_{exp} = 7813 Da), its acetylated form (MW_{exp} = 7855 Da), full length K_7NH_2Y-Z-domain (MW_{exp} = 7944 Da) and its acetylated form (MW_{exp} = 7986 Da), respectively. Importantly, no K_7Y-Z-domain was detected (MW_{exp} = 7929 Da for the full length form). Together, the studies with the Z-domain demonstrate that the evolved RS is specific for NH_2Y and is efficient at its incorporation into this target protein.

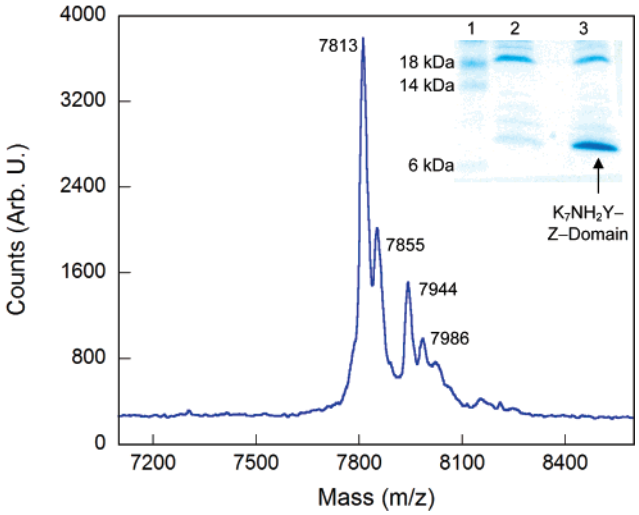

Figure 2. MALDI-TOF MS and SDS PAGE analysis of K_7NH_2Y-Z-domain. MALDI-TOF MS of purified K_7NH_2Y-Z-domain obtained under positive ionization mode. The *m*/*z* $[M + H]^+$ are indicated for the main peaks in the spectrum. They correspond to N-terminally cleaved Met form of K_7NH_2Y-Z-Domain (exp. 7814) and its acetylated form (exp. 7856), full-length K_7NH_2Y-His-Z-Domain (exp. 7945) and its acetylated form (exp. 7987). The inset shows the SDS gel of purified Z-domain after expression in the absence (lane 2) or presence (lane 3) of NH_2Y. The arrow designates the K_7NH_2Y-Z-domain band. Protein ladder and corresponding MW are shown in lane 1.

Expression and Purification of NH_2Y-α2s. Having evolved an NH_2Y-specific RS and confirmed the efficiency and fidelity of NH_2Y insertion, we next sought an overexpression system for α2 that is compatible with the plasmid/host requirements for NH_2Y incorporation. Several different growth conditions and expression systems were investigated in an effort to maximize α2 production and NH_2Y insertion at residue 730. Growth under anaerobic conditions or in the presence of hydroxyurea was investigated to minimize the reaction of wt β2 with NH_2Y-α2, which could lead to premature trapping of an $NH_2Y\cdot$ and destruction of the probe. In the former case, the anaerobic class III RNR is operative in *E. coli* and therefore wt class I β2 is not expressed.[1,74] In the latter case, presence of hydroxyurea leads to reduction of the essential $Y_{122}\cdot$ in class I β2 so that it cannot react with NH_2Y-α2.[75,76] Temperature manipulation was also investigated to minimize inclusion bodies.

Three different expression systems were investigated (see Supporting Information for details): (1) pBK-NH_2Y-RS/pBAD-*nrdA*, (2) pBK-NH_2Y-RS/pMJ1-*nrdA* and (3) pAC-NH_2Y-RS/

(69) Wang, L.; Schultz, P. G. *Chem. Biol.* **2001**, *8*, 883.
(70) Liu, D. R.; Schultz, P. G. *Proc. Natl. Acad. Sci. U.S.A.* **1999**, *96*, 4780.
(71) Zhang, Y.; Wang, L.; Schultz, P. G.; Wilson, I. A. *Protein Sci.* **2005**, *14*, 1340.
(72) Turner, J. M.; Graziano, J.; Spraggon, G.; Schultz, P. G. *Proc. Natl. Acad. Sci. U.S.A.* **2006**, *103*, 6483.
(73) Nilsson, B.; Moks, T.; Jansson, B.; Abrahmsen, L.; Elmblad, A.; Holmgren, E.; Henrichson, C.; Jones, T. A.; Uhlen, M. *Protein Eng.* **1987**, *1*, 107.
(74) Fontecave, M.; Mulliez, E.; Logan, D. T. *Prog. Nucleic Acid Res. Mol. Biol.* **2002**, *72*, 95.
(75) Rosenkranz, H. S.; Garro, A. J.; Levy, J. A.; Carr, H. S. *Biochim. Biophys. Acta* **1966**, *114*, 501.
(76) Karlsson, M.; Sahlin, M.; Sjöberg, B.-M. *J. Biol. Chem.* **1992**, *267*, 12622.

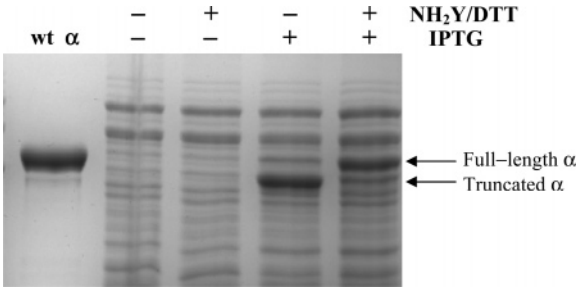

Figure 3. Expression of $Y_{731}NH_2Y$-α2. Cells were grown in the presence or absence of IPTG and NH_2Y/DTT as indicated and the level of expression assessed by SDS PAGE. The position of protein bands for full-length α and truncated α are denoted by arrows.

pMJ1-*nrdA* (see Table 1). With system 1, expression of full-length α2 at levels 1.5-fold above endogenous α2 were observed. With system 2, only truncated α2 was observed, and with system 3 overproduction of truncated α2 was accompanied by expression of full-length α2 that was similar to endogenous levels of α2 (data not shown). The failed or low levels of expression may be due to limiting $mutRNA_{CUA}$ inside the cell and/or the low levels of expression of α2 from the pBAD-*nrdA* and the pMJ1-*nrdA*.

The recent report of successful expression and incorporation of unnatural amino acids into *E. coli* nitroreductase using pTrc,[77] prompted us to investigate the pAC-NH_2Y-RS/ pTrc-*nrdA* expression system. The pTrc-*nrdA* vector carries the α2 gene under control of the *trp/lac* (*trc*) promoter with the amber stop codon at the desired residue.[78] Importantly, pAC-NH_2Y carries six copies of $mutRNA_{CUA}$, increasing the concentration of the cognate tRNA inside the cell.[63]

Expression of wt α2 from pTrc-*nrdA* was examined first. Overproduction and subsequent purification gave 10 mg of pure α2 per g of wet cell paste. This expression level is 2−4× greater than the expression of α2 from pMJ1, which has been routinely used in our lab to express α2 and α2 mutants (data not shown). In addition, the specific activity of α2 was similar to that produced from pMJ1-*nrdA* (2500 nmol/min·mg).

Expression of $Y_{731}NH_2Y$-α2 in DH10B cells doubly transformed with pAC-NH_2Y-RS and pTrc-*nrdA* is shown in Figure 3. In the presence of the IPTG inducer and NH_2Y/DTT, the amber stop codon is suppressed and NH_2Y-α2 is overexpressed. In the absence of NH_2Y, overproduction of only truncated α2 is observed. Finally, in the absence of inducer IPTG and NH_2Y, no overexpression of α2 occurs. A similar profile was obtained for the expression of $Y_{730}NH_2Y$-α2 (Figure S1). Purification of NH_2Y-α2 using dATP affinity chromatography gives 4−6 mg of the target protein per L culture in >90% homogeneity.[55,62] The mutant proteins behaved similarly to wt α2 during the purification procedure (Figure S2).

Reaction of NH_2Y-α2s with wt *β*2, CDP, and ATP Monitored by EPR Spectroscopy. The availability of NH_2Y-α2s has allowed us to assess the participation of Y_{730} and Y_{731} in radical propagation across the *β*2−α2 interface. The experimental design is based on the radical trapping method previously established with DOPA-*β*2.[38,39] In this method, a stable radical is trapped with an unnatural Y analogue that is more easily oxidized than Y. If the trapping requires the presence of *β*2, substrate, and allosteric effector, then it provides direct evidence for redox activity of that residue during radical propagation. Lack of radical formation may indicate that the residue is not redox-active or that the oxidized product is unstable. We proposed that the ease of oxidation of NH_2Y (*E*° is 190 mV lower than Y at pH 7) would lead to generation of an NH_2Y· allowing its detection by UV−vis and EPR methods.[51] Unfortunately, spectroscopic characterization of NH_2Y· has not been previously reported.

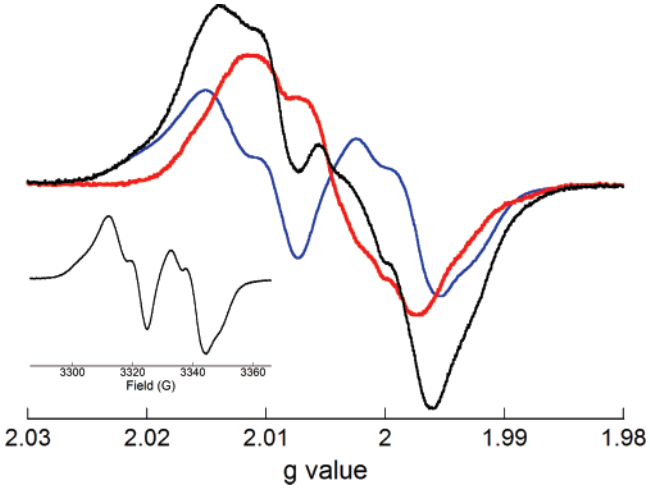

Figure 4. Reaction of $Y_{730}NH_2Y$-α2/ATP with wt *β*2/CDP monitored by EPR spectroscopy. The reaction components were mixed at 25 °C to yield final concentrations of 20 *μ*M $Y_{730}NH_2Y$-α2*β*2, 1 mM CDP, and 3 mM ATP. After 10 s, the reaction was quenched in liquid N_2 and the EPR spectrum (black) was subsequently recorded at 77 K. Unreacted Y_{122}· (blue, 47% of total spin), was subtracted to reveal the spectrum of NH_2Y_{730}· (red, 53% of total spin). The inset shows the reaction of $Y_{730}NH_2Y$-α2 with wt *β*2 in the absence of CDP/ATP.

On the basis of our studies on DOPA-*β*2,[38] we anticipated that the NH_2Y· might be stabilized to some extent by the protein environment. With DOPA-*β*2, maximal amounts of DOPA· were generated by 5 s, which was stable for 2.5 min[38,39] Thus, $Y_{730}NH_2Y$-α2 (or $Y_{731}NH_2Y$-α2) was mixed with wt *β*2, substrate (CDP), and effector (ATP), incubated at 25 °C for variable periods of time (10 s to 12 min), and quenched manually in liquid N_2. EPR spectra of these reactions revealed a new signal that was present in maximal amounts at the 10 s time point (Figure 4). A control in the absence of CDP and ATP, revealed only Y_{122}· (Figure 4, inset). Thus formation of the new signal is controlled by the presence of substrate and effector as previously observed with similar studies on DOPA-*β*2.[38]

The observed spectrum is a composite of at least two species: unreacted Y_{122}· and the putative NH_2Y_{730}·. To reveal the features of the new radical(s), the spectrum of the Y_{122}·[14] with distinct, well characterized low field features was subtracted from the composite signal. The resulting nearly isotropic signal (Figure 4, red trace) has an apparent g_{av} of 2.0043 and a peak-to-trough width of 24 G.[79] We ascribe this new signal to NH_2Y_{730}·.

Spin quantitation at the 10 s time point revealed that 8% of total initial spin (relative to starting Y_{122}·) had been lost. Of the remaining spin, 47% is associated with Y_{122}· and 53% with the new signal. To further characterize this signal, power

(77) Jackson, J. C.; Duffy, S. P.; Hess, K. R.; Mehl, R. A. *J. Am. Chem. Soc.* **2006**, *128*, 11124.
(78) Amann, E.; Ochs, B.; Abel, K. J. *Gene* **1987**, *61*, 41.
(79) A more detailed analysis of the new radical species will be presented elsewhere.

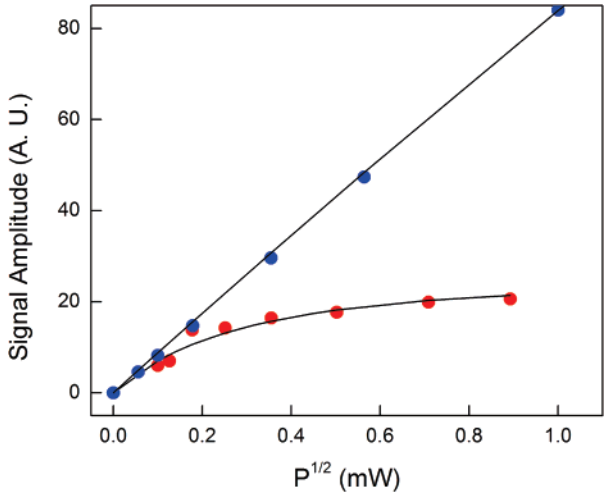

Figure 5. Microwave power dependence of Y_{122}• and NH_2Y_{730}• signal intensities. The EPR spectrum of the Y_{122}• and NH_2Y_{730}• was recorded as a function of microwave power, and the integrated intensity of each signal was plotted against the square root of power. Black lines represent fits to the data using eq 1[80] and yield $P_{1/2}$ of 28 ± 4 mW (b = 1.3 ± 0.2) and 0.42 ± 0.08 mW (b = 1.2 ± 0.2) for Y_{122}• (blue) and NH_2Y_{730}• (red), respectively.

saturation studies were carried out. The Y_{122}• is adjacent to the diferric cluster, which dramatically alters its relaxation properties. If the new radical is in fact located within α2, >35 Å removed from the diferric cluster as indicated by the docking model, then its $P_{1/2}$ would be markedly reduced. The results of power dependence experiments are shown in Figure 5. The data were fit to eq 1,[80] where K is a sample and instrument dependent scaling factor, P is the microwave power, b is indicative of homogeneous (b = 3) or inhomogeneous (b = 1) spectral broadening and $P_{1/2}$ is the microwave power at half saturation of the EPR signal.[79,81] For the Y_{122}•, a $P_{1/2}$ of 28 ± 4 mW was determined, similar to previous measurements.[81,82] The saturation profile of the new signal gave a $P_{1/2}$ of 0.42 ± 0.08 mW consistent with a radical distant from the diiron center.

$$\text{signal amplitude} = \frac{K \times (\sqrt{P})}{[1 + (P/P_{1/2})]^{0.5 \times b}} \qquad (1)$$

Similar experiments have also been carried out with Y_{731}-NH_2Y-α2. A new signal, the putative NH_2Y_{731}•, is also observed *only* in the presence of CDP/ATP (Figure S3). Subtraction of the Y_{122}• spectrum reveals a spectrum that is similar, but not identical, to that of NH_2Y_{730}• (Figure 6). The nearly isotropic signal associated with NH_2Y_{731}• consists of a g_{av} of 2.0044 and a peak-to-trough width of 22 G. At the 10 s time point, 14% of total initial spin has been lost. Of the remaining spin, 45% is associated with NH_2Y_{731}• and 55% with Y_{122}•.

Kinetics of NH_2Y•-α2 Formation Monitored by SF UV−Visible Spectroscopy. Pre-steady-state experiments were carried out to assess whether NH_2Y•-α2 formation occurs with a rate constant fast enough to be competent in nucleotide reduction in wt RNR. Previous steady state and pre-steady-state kinetic

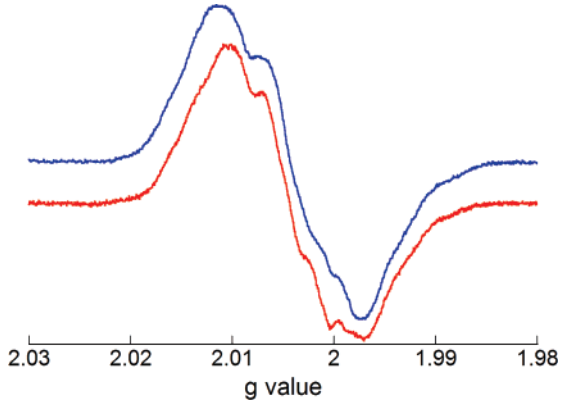

Figure 6. Comparison of the NH_2Y_{730}• (blue, Figure 4) and NH_2Y_{731}• (red, Figure S3).

analysis of *E. coli* RNR monitoring nucleotide reduction have shown that radical propagation is preceded by a slow conformation change.[83] This slow physical step masks intermediates that form in the propagation process. In the presence of CDP/ATP, and at concentrations of α2 and β2 used in the present study, the rate constant for this conformational change varies from ~4 to 17 s^{-1}.[83] The steady-state rate constant for dCDP formation is on the order of 2 s^{-1} and is thought to be limited by re-reduction of the active site disulfide that accompanies dCDP formation or by a conformational change associated with re-reduction. In previous studies with DOPA-β2, α2, and CDP/ATP, DOPA• formation occurred in two fast kinetic phases (38.0 and 6.8 s^{-1}) and a slow phase (0.7 s^{-1}). Thus, the two fast phases in the DOPA-β2 experiments, and potentially the third phase,[84] were kinetically competent with respect to the conformational change, which limits dCDP formation in the first turnover.[83]

To monitor changes in the concentration of NH_2Y•, its spectrum and extinction coefficient must be determined. Our initial assumption was that its UV−vis spectrum would be similar to that of DOPA• (λ_{max} at 315 nm and $\epsilon \approx$12000 M^{-1} cm^{-1}).[38,85] The extinction coefficients associated with Y_{122}• between 310 and 365 nm are low ($\epsilon \approx$ 500−1900 M^{-1} cm^{-1}) and can be used in spectral deconvolution.[66,67] Thus, using SF spectroscopy, we carried out a point-by-point analysis of the UV−vis properties of the new radical. $Y_{730}NH_2Y$-α2 (or Y_{731}-NH_2Y-α2) and ATP in one syringe was mixed with wt β2 and CDP from a second syringe, and the absorbance was monitored from 305 to 365 nm in 5 nm intervals. The absorbance change at 1.5 s at each λ, corrected for the absorption by the Y_{122}•,[66,67] was then plotted against the λ. The results are shown in Figure 7 and indicate that NH_2Y_{730}• and NH_2Y_{731}• have similar but distinct absorption profiles. The UV−vis spectrum of NH_2Y_{730}• consists of a broad feature with a λ_{max} at 325 nm ($\epsilon \approx$ 10500 M^{-1} cm^{-1}). The NH_2Y_{731}• spectrum exhibits a λ_{max} at 320 nm ($\epsilon \approx$ 11000 M^{-1} cm^{-1}) and a more defined shoulder at 350 nm. The extinction coefficients for NH_2Y•-α2s were determined using ϵ for Y_{122}• at 410 nm[68] and the assumption that the loss of each mole of Y_{122}• leads to formation of one mole of NH_2Y•.

(80) Chen-Barrett, Y.; Harrison, P. M.; Treffry, A.; Quail, M. A.; Arosio, P.; Santambrogio, P.; Chasteen, N. D. *Biochemistry* **1995**, *24*, 7847.
(81) Sahlin, M.; Petersson, L.; Gräslund, A.; Ehrenberg, A.; Sjöberg, B.-M.; Thelander, L. *Biochemistry* **1987**, *26*, 5541.
(82) Gerfen, G. J.; van der Donk, W. A.; Yu, G.; McCarthy, J. R.; Jarvi, E. T.; Matthews, D. P.; Farrar, C.; Griffin, R. G.; Stubbe, J. *J. Am. Chem. Soc.* **1998**, *120*, 3823.
(83) Ge, J.; Yu, G.; Ator, M. A.; Stubbe, J. *Biochemistry* **2003**, *42*, 10071.
(84) Rapid chemical quench studies monitoring dCDP formation with intein-generated wt β2 no longer show a burst of dCDP formation (as with wt β2) but exhibit a single rate constant of ~1 s^{-1}(M. Seyedsayamdost, J. Stubbe, unpublished results). Thus, the slow phase observed with DOPA-β2 could also be kinetically competent in turnover.
(85) Craw, M.; Chedekel, M. R.; Truscott, T. G.; Land, E. J. *Photochem. Photobiol.* **1984**, *39*, 155−159.

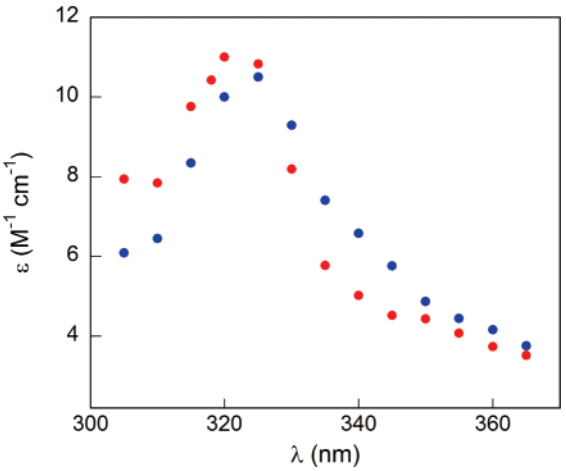

Figure 7. Point-by-point reconstruction of the UV−vis spectrum of NH_2Y_{730}• (blue dots) and NH_2Y_{731}• (red dots). Prereduced $Y_{730}NH_2Y$-α2 and ATP in one syringe were mixed with wt β2 and CDP from another syringe, yielding final concentrations of 10 μM, 3 mM, 10 μM, and 1 mM, respectively. With $Y_{731}NH_2Y$-α2, the reaction was carried out at final concentrations of 9 μM $Y_{731}NH_2Y$-α2β2, 1 mM CDP, and 3 mM ATP. The absorption change was monitored in 5 nm intervals; at each λ, 2−4 time courses were averaged and corrected for the absorption of Y_{122}• using previously determined ε in this spectral range.[66,67] The corrected ΔOD was converted to ε,[68] which was then plotted against λ.

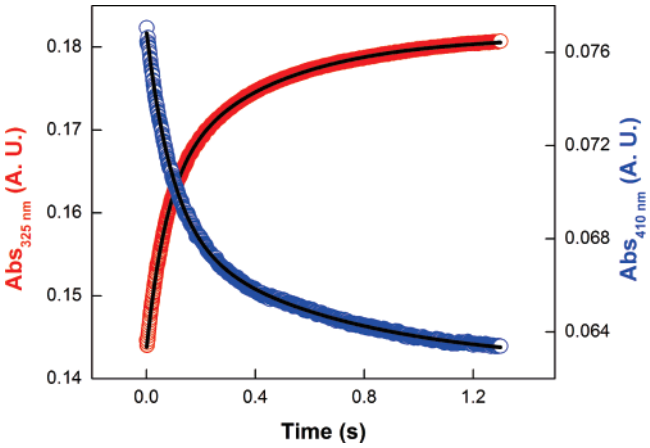

Figure 8. SF kinetics of NH_2Y_{730}• formation. Prereduced $Y_{730}NH_2Y$-α2 (20 μM) and CDP (2 mM) in one syringe were mixed in a 1:1 ratio with β2 (20 μM) and ATP (3 mM) from another syringe. A total of 7 traces were averaged at 325 and 410 nm monitoring NH_2Y_{730}• formation (red) and Y_{122}• disappearance (blue), respectively. Black lines indicate biexponential fits to the data (see Table 2 for kinetic parameters).

SF UV−vis experiments carried out to monitor the kinetics of loss of Y_{122}• (410 nm) and formation of NH_2Y• (325 nm) are shown in Figure 8 for $Y_{730}NH_2Y$-α2. At 410 nm, biexponential kinetics with rate constants of 12.0 ± 0.1 s^{-1} and 2.4 ± 0.1 s^{-1} were observed, similar to rate constants obtained for formation of NH_2Y• at 325 nm (13.6 ± 0.1 and 2.5 ± 0.1 s^{-1}). Analogous experiments carried out with $Y_{731}NH_2Y$-α2 showed that loss of Y_{122}• occurred biexponentially (17.3 ± 0.2 and 2.3 ± 0.1 s^{-1}) concomitant with formation of NH_2Y_{731}• (21.0 ± 0.1 s^{-1} and 3 ± 0.1 s^{-1}, Figure S4). The rate constants and amplitudes for both reactions are summarized in Table 2. A control experiment was carried out in the absence of substrate and effector with $Y_{730}NH_2Y$-α2 (or $Y_{731}NH_2Y$-α2) and β2. As indicated by EPR experiments, no loss of Y_{122}• or formation of NH_2Y• occurred under identical conditions (data not shown).

Table 2. Summary of Kinetic Data for Formation of NH_2Y•-α2

RNR subunits	CDP/ATP	first phase k_{obs} (s^{-1})[a], Ampl[b] (%)	second phase k_{obs} (s^{-1})[a], Ampl[b] (%)
$Y_{730}NH_2Y$-α2β2	no	*c*	*c*
$Y_{730}NH_2Y$-α2β2	yes	12.8 ± 0.8, 20 ± 1	2.5 ± 0.1, 19 ± 1
$Y_{731}NH_2Y$-α2β2	no	*c*	*c*
$Y_{731}NH_2Y$-α2β2	yes	19.2 ± 1.8, 24 ± 1	2.7 ± 0.4, 11 ± 1

[a] The rate constants reported are the averages of those measured at 410 nm (for Y_{122}• loss) and at 320 nm (for NH_2Y_{731}• formation) or 325 nm (for NH_2Y_{730}• formation). The error corresponds to the standard deviation between these two measurements. [b] Ampl, amplitude; the amount of Y_{122}• trapped in each kinetic phase is indicated as a % of total initial Y_{122}•. Because the determination of ε for NH_2Y• was based on that of Y_{122}•, the amplitudes at 410 nm and 320 or 325 nm are nearly identical. In this case, the estimated error is due to instrumental factors. [c] No changes observed.

Table 3. Monitoring the Activity of NH_2Y-α2s by Measuring Deoxynucleotide and N• Formation

α2 variant	spectrophotometric RNR assay (wt %)[a]	radioactive RNR assay (wt %)[a]	N_3ADP assay (% N• at 20 s,[b] % N• vs initial Y_{122}•[c])
wt α2	100[a]	100[a]	52
$Y_{730}NH_2Y$-α2	4 ± 0.3	4 ± 0.5	19 ± 2,[b] 15 ± 2[c]
$Y_{731}NH_2Y$-α2	7 ± 1	7 ± 0.5	20 ± 2,[b] 15 ± 2[c]

[a] The activity is reported as % of wt activity, which was 2500 nmol/min•mg. The error is the standard deviation from 3 independent measurements for the spectrophotometric assay and 2 independent measurements for the radioactive assay. [b] The amount of N• is indicated as % of total spin at 20 s; the error is associated with EPR spin-quantitation methods. [c] The amount of N• is indicated as % of total initial Y_{122}•; the error is associated with EPR spin quantitation.

As noted above, the fast rate constants observed with the NH_2Y-α2s are kinetically competent in RNR turnover. Thus studies with these mutants provide the first direct evidence for their involvement in radical propagation. The slow rate constant, also observed in the DOPA-β2 experiments, is similar to the steady-state rate constant for RNR turnover. A possible explanation for this slow phase is discussed below.

Finally, analysis of the amounts of each radical at 2 s shows that with $Y_{730}NH_2Y$-α2 and $Y_{731}NH_2Y$-α2, 39% and 35% of total initial Y_{122}• is consumed, respectively. In contrast with the DOPA-β2, the NH_2Y• is less stable. The instability needs to be assessed in detail and requires kinetic analysis using rapid freeze quench methods to unravel its mechanistic implications.

Activities of NH_2Y-α2s. Recently, using a series of F_nY_{356}-β2s, we found a correlation between nucleotide reduction activity and the reduction potential of residue 356, when its potential was 80 to 200 mV higher than that of tyrosine.[40,43] The reduction potential of DOPA is 260 mV lower than that of Y (pH 7) and with DOPA-β2,[38] deoxynucleotide formation was below our lower limit of detection. With NH_2Y-α2, the potential of NH_2Y is 190 mV lower than that of Y (pH 7).[51] To test whether this energy barrier would be large enough to shut down radical transfer to C_{439}, and therefore nucleotide reduction, activity assays were performed on NH_2Y-α2s.

Activity was determined by monitoring dCDP formation indirectly (spectrophotometric assay) or directly (radioactive assay). The activities determined using these assays are summarized in Table 3. The results show nucleotide reduction activity for $Y_{730}NH_2Y$-α2 and $Y_{731}NH_2Y$-α2 that is 4% and 7% that of wt α2, respectively. The observed activity may be inherent to NH_2Y-α2s; on the other hand, it may be ascribed to co-purifying endogenous wt α2 or to wt α2 generated by the

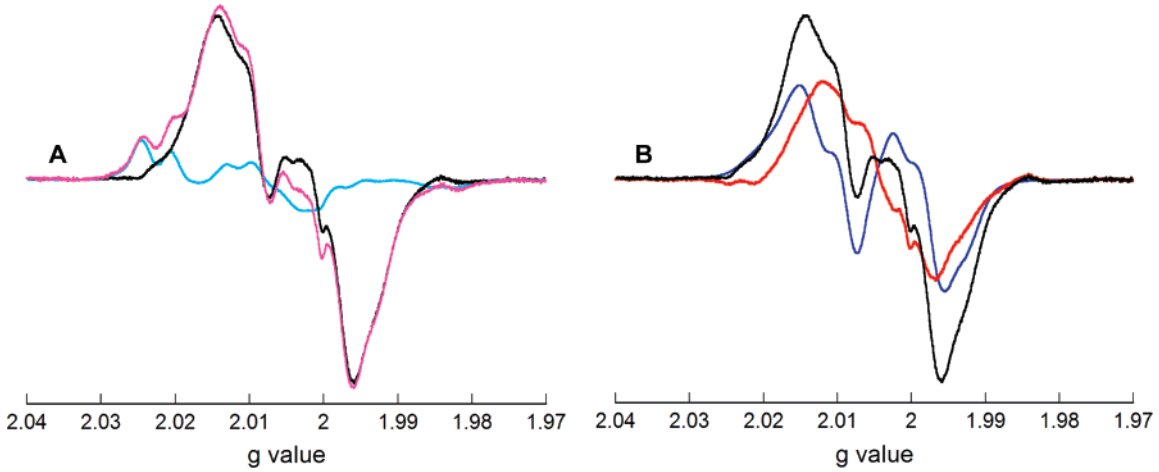

Figure 9. Formation of N· from N_3ADP upon incubation with $Y_{730}NH_2Y$-α2, β2, and dGTP. The reaction contained final concentrations of 20 μM Y_{730}-NH_2Y-α2β2 (1.2 Y_{122}·/β2), 1 mM N_3ADP, and 0.25 mM dGTP. After 20 s, it was freeze-quenched in liquid N_2, and its EPR spectrum was recorded. (A) Subtraction of N· (aqua, 19% of total spin) from the observed spectrum (lavender) yields the black trace, which contains the Y_{122}· and NH_2Y_{730}· signals. (B) Subtraction of Y_{122}· (blue, 43% of total) from the resulting spectrum in (A) reveals the spectrum of NH_2Y_{730}· (red, 39% of total spin). See Table 4 for quantitation of the concentration of each radical species.

host cell as a result of amber codon suppression with Tyr-loaded $mutRNA_{CUA}$ in place of NH_2Y-loaded $mutRNA_{CUA}$.

To distinguish between these two options, assays with N_3-ADP were carried out. N_3ADP is a mechanism-based inhibitor of class I RNRs which generates a moderately stable N-centered radical (N·) covalently bound to the nucleotide and a cysteine in the active site of α2.[28−31,86] This radical may be used as a reporter of the ability of NH_2Y· to generate a C_{439}· and initiate chemistry on the nucleotide. Previous studies of the inactivation of wt α2β2 by N_3ADP/dGTP suggest that on a 20 s time scale, 50−60% of the initial Y_{122}· is lost leading to formation of an equivalent amount of N·.[30,62] Therefore, if the activity observed with NH_2Y-α2s is indicative of wt α2, ∼2% and ∼3.5% of total initial Y_{122}· would be expected to form a N· with Y_{730}-NH_2Y-α2 and $Y_{731}NH_2Y$-α2, respectively.

Assays with N_3ADP were carried out by mixing each NH_2Y-α2 (or wt α2) and dGTP with wt β2 and N_3ADP. After 20 s the reaction was hand-quenched in liquid N_2. The EPR spectrum obtained for $Y_{730}NH_2Y$-α2 is shown in Figure 9. The observed spectrum is a combination of at least three radicals: Y_{122}·, NH_2Y_{730}·, and N·. The spectrum can be deconvoluted using the differences in spectral widths and the unique spectral features within these regions (Figure 10). Thus, the data were analyzed by first subtracting the N· spectrum, which contains the broadest of the three signals. The resulting spectrum was then subjected to fractional subtraction of the Y_{122}· component, yielding the NH_2Y_{730}· signal. The concentration of each of the radicals was determined using standard EPR quantitation methods.[65]

The results from this quantitative analysis are shown in Table 4. They show that 18% of the total spin has been lost at the 20 s time point. Of the remaining spin, 19 ± 2% is associated with N·, 43% is Y_{122}·, and 39% is NH_2Y_{730}·. Accounting for the lost spin after 20 s, 15 ± 2% of total initial Y_{122}· (i.e., at t = 0) leads to N· formation. With $Y_{731}NH_2Y$-α2 (Figure S5 and Table 4), 25% of the total spin is lost after 20 s with 20 ± 2% present as N·, 41% as Y_{122}· and 39% as NH_2Y_{731}·. Accounting for the lost spin after 20 s, 15 ± 2% of total initial Y_{122}· leads to formation of N·. Therefore, with both mutants, the amount of N· observed exceeds the 2% or 3.5% N· (for $Y_{730}NH_2Y$-α2 and $Y_{731}NH_2Y$-α2, respectively), expected if the steady state activity was due to contaminating wt α2. These results strongly suggest that NH_2Y-α2s are competent in C_{439}· formation and thus nucleotide reduction.

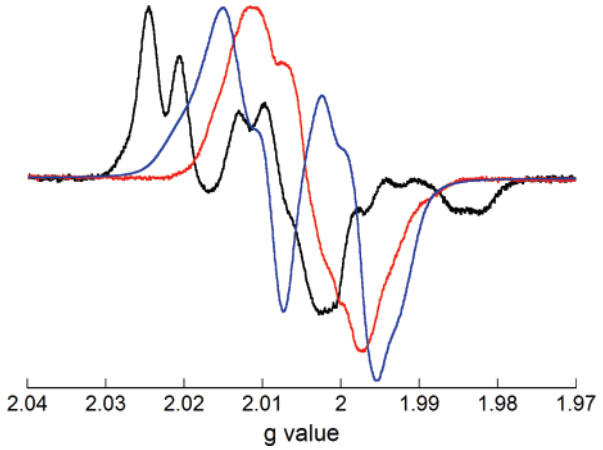

Figure 10. Spectral comparison of N· (black), Y_{122}· (blue), and NH_2Y_{730}· (red). The distinct features of N· and Y_{122}·, on the low field side of the spectrum, facilitate in deconvolution of the complex spectra in Figures 4, 9, S3, and S5.

Table 4. Analysis of the Reaction of wt α2 or NH_2Y-α2s with β2 and N_3ADP/dGTP at 20 s[a]

α2 variant	$[spin]_T$ (μM)[b]	[N·] (μM)	$[Y_{122}$·] (μM)	$[NH_2Y$·] (μM)
wt α2	22.9	11.9	11.0	
$Y_{730}NH_2Y$−α2	19.5	3.7	8.4	7.6
$Y_{731}NH_2Y$−α2	18.1	3.6	7.5	7.1

[a] The error associated with EPR quantitation was ∼10%. [b] In each case, the initial [Y_{122}·] was 24 μM.

Discussion

Generation of $Y_{730}NH_2Y$-α2 and $Y_{731}NH_2Y$-α2. In this study, we have evaluated the proposed roles for residues Y_{730} and Y_{731} in radical propagation, by site-specifically replacing them with NH_2Y (Figure 1). We employed the in vivo suppressor tRNA/RS method, which has been pioneered[46] and

(86) van der Donk, W. A.; Stubbe, J.; Gerfen, G. J.; Bellew, B. F.; Griffin, R. G. *J. Am. Chem.* Soc. **1995**, *117*, 8908.

developed[47−50] by the Schultz lab and promises to have an immense impact on protein biochemistry. Using this technology, we evolved the desired tRNA/RS pair, which allowed us to generate $Y_{730}NH_2Y$-α2 and $Y_{731}NH_2Y$-α2 in yields of 4−6 mg per g of wet cell paste. The large size of α2 (172 kDa) and the small size difference between NH_2Y and Y have precluded quantitative assessment of NH_2Y incorporation into α2 by direct ESI or MALDI TOF mass spectrometric methods. Analytical methods using LC/MS of tryptic digests of this 172 kDa protein, to evaluate levels of NH_2Y relative to Y in NH_2Y-α2s, are currently being developed. Nevertheless, our studies with the model Z-domain protein indicate that incorporation of NH_2Y is efficient and specific. In addition, evaluation of our NH_2Y-α2 preparations, using N_3ADP and dCDP assays, also suggest the presence of low levels of wt α2.

The ability to incorporate NH_2Y site-specifically into proteins will be of general use. Our characterization of the UV−vis and EPR spectroscopic properties of the NH_2Y• should allow NH_2Y to serve as a probe for enzymes that are thought to employ transient Y•s in catalysis or in electron transfer between metal centers. In addition, Francis and colleagues have recently shown that NH_2Y may be derivatized with fluorescent dyes.[87,88] Thus, NH_2Y may also be utilized as a tool for site-specifically appending probes of interest to the target protein.

Structural Assignment of the New Radical. When NH_2Y-α2s are reacted with β2, in the presence of CDP/ATP, a new EPR-active signal is observed. As noted above, however, neither UV−vis nor EPR spectral properties of the NH_2Y• had previously been reported. The assignment of our new signal to NH_2Y• is based on SF UV−vis and EPR spectroscopic measurements in conjunction with knowledge of the properties of DOPA, catechol, and *o*-aminophenol radicals.[89,90] First, point-by-point reconstruction of the new radical's UV−vis spectrum by SF methods reveals an absorption spectrum similar to DOPA•, which is expected based on the structural similarity between these two amino acids. Second, subtraction of the Y_{122}• EPR spectrum from the observed EPR signal, yields a spectrum with a g_{av} of 2.0043 ± 0.0001 which is typical of organic radicals. The small hyperfine couplings (<10 G) from the ring protons and from the amine nitrogen are similar to those previously reported for *o*-aminophenol radicals.[89] Third, information about the location of the new radical relative to the diferric cluster has been obtained by power saturation studies. These studies show that Y_{122}• saturates with a $P_{1/2}$ of 28 mW owing to its vicinity to the diferric cluster (4.6 Å to the nearest iron in the cluster).[19] Mechanism-based inhibitors that covalently label the active site of α2, >35 Å from the cluster, have $P_{1/2}$ values of 0.16 mW.[82] The new radical has a $P_{1/2}$ of 0.42 ± 0.08 mW consistent with a species distant from the diiron center. These data together strongly suggest that the new radical is NH_2Y• (Scheme 1).[91] High-field EPR and ENDOR experiments, isotopic labeling studies with ^{15}N and ^{2}H in conjunction with computational studies are in progress to further support this assignment.

Kinetics of NH_2Y•-α2 Formation. SF kinetic studies give rate constants of 12.8 and 2.5 s^{-1} for $Y_{730}NH_2Y$-α2, and 19.2 and 2.7 s^{-1} for $Y_{731}NH_2Y$-α2. The fast rate constant is indicative of a rate-determining conformational change, which has previously been found to precede radical propagation in wt β2, under single turnover conditions.[83] Thus, formation of NH_2Y• occurs in a kinetically competent fashion at the expense of the Y_{122}•.[38] Further, as with DOPA, NH_2Y acts as a conformational probe and allows direct detection of this physical step, reporting on the regulatory state of the NH_2Y-α2β2 complex. The slow rate constant observed in these kinetic studies has also been observed when monitoring $DOPA_{356}$• formation (0.4 to 0.8 s^{-1} with different substrate/effector pairs).[38,84] These rate constants are all in the same range, similar to the turnover number of RNR at the protein concentrations used in these experiments. Our previous studies have suggested that in the steady state, re-reduction of the disulfide or a conformational change associated with this process is rate-limiting. If the latter is the case, then this rate constant of 2−3 s^{-1}, might be indicative of the slow conversion of one form of RNR into the more active form. Alternatively, incorporation of NH_2Y could result in α2 with two conformations of the tyrosine analogue that do not interconvert rapidly or two different conformations of the α2 itself. The separate kinetic phases for NH_2Y• formation indicate that these two conformations do not interconvert on the time scale of the SF experiment. Additional kinetic analysis is required to further assign the nature of the slow rate constant observed.

Activity Assays of NH_2Y-α2s. Steady-state turnover measurements show the ability of both mutant proteins to produce dNDPs. As noted above, this activity could be associated with endogenous wt α2, which co-purifies with NH_2Y-α2s, or with wt α2 which is generated by suppression of the amber codon with Tyr-loaded $mutRNA_{CUA}$ in place of NH_2Y. Alternatively, the activity may be inherent to NH_2Y-α2s.

To distinguish between these options, experiments with the mechanism-based inhibitor N_3ADP were carried out. The results indicate 15 ± 2% N• formation with $Y_{730}NH_2Y$-α2 and Y_{731}-NH_2Y-α2. These values exceed the expected 2% and 3.5%, respectively, if the steady-state turnovers were due to background levels of wt α2. Thus, the results suggest that NH_2Y-α2s are competent in deoxynucleotide production. This implies that the putative NH_2Y• is an intermediate during active radical transport. Detailed kinetic analysis on the ms time scale will further test this proposition. If true, then these observations would mark the first detection of an amino acid radical during long-range hole migration in an RNR variant that is competent in dNDP formation.

Implications for Mechanism of Oxidation. Competence in nucleotide reduction has interesting mechanistic implications for radical propagation within $Y_{730}NH_2Y$-α2. Three mechanisms may be envisioned for oxidation of C_{439} by NH_2Y_{730}•: This reaction may occur by (1) a stepwise process, that is, electron transfer followed by proton transfer, (2) an orthogonal proton-coupled electron transfer (PCET), or (3) a collinear PCET (i.e., hydrogen atom transfer, Figure 11).[92−94] The option of the

(87) Hooker, J. M.; Kovacs, E. W.; Francis, M. B. *J. Am. Chem. Soc.* **2004**, *126*, 3718.
(88) Kovacs, E. W.; Hooker, J. M.; Romanini, D. W.; Holder, P. G.; Berry, K. E.; Francis, M. B. *Bioconjug. Chem.* **2007**, *18*, 1140.
(89) Felix, C. C.; Sealy, R. C. *J. Am. Chem. Soc.* **1981**, *103*, 2831.
(90) Neta, P.; Fessenden, R. W. *J. Phys. Chem.* **1974**, *78*, 523.
(91) Previous computational studies on *o*-aminophenol have shown that the BDE of the phenolic hydroxyl group is lower than that of the amine. EPR studies on *o*-aminophenol are in line with these calculations demonstrating the presence of two N-bound protons in the oxidized state (see refs 90 and 96). Our own preliminary EPR simulations and DFT calculations also suggest that the structure of the radical is that shown in Scheme 1 (M. Seyedsayamdost, M. Bennati, J. Stubbe, unpublished results).
(92) Cukier, R. I.; Nocera, D. G. *Annu. Rev. Phys. Chem.* **1998**, *49*, 337.

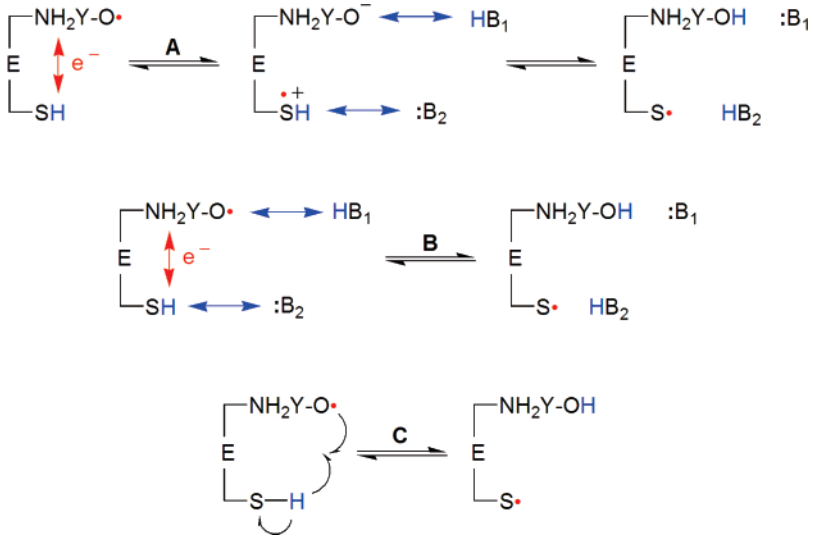

Figure 11. Mechanistic options for oxidation of C_{439} by NH_2Y_{730}•. (A) Stepwise electron transfer/proton transfer. The initial electron transfer event generates a distinct intermediate which contains a thiyl cation radical and an 3-aminotyrosinate ($NH_2Y_{730}^-$). Subsequent proton-transfer yields a neutral thiyl radical and NH_2Y_{730}. This reaction is highly disfavored (see text). (B) Orthogonal PCET. ET and proton transfer are coupled but the electron and proton have different destinations. The proton of C_{439} is transferred orthogonally to a basic residue; its electron is transferred to NH_2Y_{730}•, thus generating a C_{439}• and NH_2Y_{730}. (C) Co-linear PCET. Hydrogen-atom transfer from C_{439} to NH_2Y_{730}•. Proton and electron originate from and arrive at the same moiety.

stepwise process may be eliminated due to thermochemical bias against formation of high-energy charged intermediates in the nonpolar α2 active site as well as the insurmountable energy barrier for formation of a cysteine cation radical by the NH_2Y•/NH_2Y^- couple (Figure 11A).[93] Orthogonal PCET requires oxidation of C_{439}, which has a solution reduction potential of 1.33 V at pH 7, by a NH_2Y• which has $E°$ of 0.64 V at pH 7 (Figure 11B).[1,51] Therefore, the second option would require a thermodynamically uphill process that is unfavorable by 16 kcal/mol. The hydrogen-atom transfer mechanism, however, is thermodynamically more accessible (Figure 11C). Its feasibility is based on knowledge of the homolytic bond dissociation energies of R-SH (88−91 kcal/mol) and *o*-aminophenol, calculated to be 78−83 kcal/mol.[1,95−97] Therefore, oxidation of C_{439} by NH_2Y_{730}• by a hydrogen-atom transfer mechanism, assuming no perturbations in the protein milieu, is uphill by "only" 5−13 kcal/mol. Thus, nucleotide reduction activity in $Y_{730}NH_2Y$-α2 would thermodynamically favor a hydrogen-atom transfer mechanism for C_{439}• formation by NH_2Y_{730}•.

Interestingly, the bond dissociation energy of catechol (82−83 kcal/mol) is similar to that of *o*-aminophenol.[95] However, $DOPA_{356}$-β2 is inactive in nucleotide reduction. In the case of DOPA-β2 orthogonal PCET, the functional mechanism of oxidation at this residue (i.e., similar to Figure 11B), requires matching redox potentials for efficient radical propagation and nucleotide reduction. With, $Y_{730}NH_2Y$-α2, competence in nucleotide reduction, despite unmatched redox potentials (∼0.69 V difference), appears to be reconciled owing to a different mechanism of oxidation via hydrogen atom transfer, which appears to operate at this residue in the pathway.

In conclusion, we report evolution of a suppressor tRNA/RS pair that is specific for the unnatural amino acid NH_2Y. Site-specific insertion of NH_2Y will be useful for other systems that use Y•s in catalysis and for attaching probes of interest to a target protein. Using this technology we generated $Y_{730}NH_2Y$-α2 and $Y_{731}NH_2Y$-α2 and tested involvement of these residues in long-range radical propagation. The results demonstrate kinetically competent radical transfer from the Y_{122}• in β2 across the subunit interface and trapping of NH_2Y_{730}• or NH_2Y_{731}•. This event is triggered by binding of substrate and effector. Steady-state activity assays in conjunction with reactions with the suicide inhibitor N_3ADP indicate that $Y_{730}NH_2Y$-α2 and $Y_{731}NH_2Y$-α2 are competent in nucleotide reduction. This implicates a hydrogen-atom transfer mechanism for oxidation of C_{439} by NH_2Y_{730}•. Definitive evidence for activity of NH_2Y-α2s requires a detailed kinetic analysis of the decay of NH_2Y• and formation of N• with the mechanism-based inhibitor N_3-NDP. These studies are currently in progress.

Acknowledgment. We thank Eric Brustad, Dr. Lubica Supekova, and Jonathan Chittuluru for helpful advice during selection of NH_2Y-RS, Youngha Ryu and Roshan Perera for cloning of pAC-NH_2Y, and the National Institutes of Health, Grant GM29595 (J.S.) and Grant GM62159 (P.G.S.), for support.

Supporting Information Available: Attempts at expression of $Y_{730}NH_2Y$-α2 from vectors pBAD-*nrdA* and pMJ1-*nrdA* under various conditions, expression gel of $Y_{730}NH_2Y$-α2 with pTrc-*nrdA*, purification gels of NH_2Y-α2s, SF UV−vis characterization and 10 s EPR spectrum of the reaction of $Y_{731}NH_2Y$-α2 with β2, CDP/ATP and EPR spectra for the reaction of $Y_{731}NH_2Y$-α2/β2 with N_3ADP and dGTP. This material is available free of charge via the Internet at http://pubs.acs.org.

JA076043Y

(93) Mayer, J. M.; Rhile, I. J. *Biochim. Biophys. Acta* **2004**, *1655*, 51.
(94) Reece, S. Y.; Hodgkiss, J. M.; Stubbe, J.; Nocera, D. G. *Philos. Trans. R. Soc. London, Ser. B* **2006**, *361*, 1351.
(95) Borges dos Santos, R. M.; Martinho Simões, J. A. *J. Phys. Chem. Ref. Data* **1998**, *27*, 707.
(96) Wright, J. S.; Johnson, E. R.; DiLabio, G. A. *J. Am. Chem. Soc.* **2001**, *123*, 1173.
(97) Bakalbassis, E. G.; Lithoxoidou, A. T.; Vafiadis, A. P. *J. Phys. Chem. A* **2006**, *110*, 11151.